Dimensional scaling treatment of stability of atomic anions induced by superintense, high-frequency laser fields

Qi Wei and Sabre Kais
Department of Chemistry, Purdue University, West Lafayette, Indiana 47907, USA
and Birck Nanotechnology Center, Purdue University, West Lafayette, Indiana 47907, USA

Dudley Herschbach
Department of Physics, Texas A&M University, College Station, Texas 77843, USA

(Received 24 May 2007; accepted 9 July 2007; published online 4 September 2007)

We show that dimensional scaling, combined with the high-frequency Floquet theory, provides useful means to evaluate the stability of gas phase atomic anions in a superintense laser field. At the large-dimension limit ($D\rightarrow\infty$), in a suitably scaled space, electrons become localized along the polarization direction of the laser field. We find that calculations at large D are much simpler than $D=3$, yet yield similar results for the field strengths needed to bind an "extra" one or two electrons to H and He atoms. For both linearly and circularly polarized laser fields, the amplitude of quiver motion of the electrons correlates with the detachment energy. Despite large differences in scale, this correlation is qualitatively like that found between internuclear distances and dissociation energies of chemical bonds. © *2007 American Institute of Physics*. [DOI: 10.1063/1.2768037]

I. INTRODUCTION

The stability of atomic and molecular anions in the gas phase is pertinent to many phenomena and has been extensively studied.[1,2] Many singly charged negative atomic ions are known, but only recently have theoretical calculations, supported by experimental results, clearly excluded the existence of any stable gas phase doubly negatively charged atomic ion.[3] Such atomic anions might, however, be stable in very intense magnetic fields.[4] Multiply charged gas phase molecular anions have been observed, but most involve many atoms.[5] The question of the smallest molecule that can stably bind two or more excess electrons remains open.[6,7]

Another perspective has emerged from theory revealing exotic and often paradoxical electronic properties of atoms induced by high-frequency superintense radiation fields.[8] For this realm, a particularly striking aspect is that the ionization probability decreases as laser intensity increases.[9] Calculations employing the Floquet theory have predicted the stabilization of multiply charged anions of hydrogen[10] and doubly charged anions of helium and lithium atoms.[11] As yet, such stabilization has not been demonstrated experimentally, except for atoms initially prepared in a Rydberg state.[12]

The predicted stabilization of atomic anions is accompanied by the splitting of the electronic charge distribution into lobes governed by the polarization of the laser field. This localization of the electrons markedly reduces encounters with the nucleus as well as electron correlation and hence suppresses autoionization.[9,13] Such pronounced localization is also a feature seen in a pseudoclassical limit of dimensional scaling theory as applied to an electronic structure.[14] In this paper, in addition to extending results employing calculations for $D=3$, we examine the large-D limit for the Floquet theory. We find that it indeed provides a useful approximation for evaluating the detachment energy as a function of the laser field parameters. As the large-D limit requires far simpler computations than are required for $D=3$, it may facilitate examining prospects for laser induced stabilization of molecular anions.

II. LASER ATOM INTERACTION

We consider a high-frequency monochromatic electric field with amplitude E_0 and frequency ω incident on an N-electron atom.[15] In the dipole approximation, each electron is subjected in the same field and undergoes quiver oscillations $\alpha(t)$ along a trajectory given by

$$\alpha(t) = \alpha_0(\mathbf{e}_1 \cos \omega t + \mathbf{e}_2 \tan \delta \sin \omega t), \tag{1}$$

where the quiver amplitude is $\alpha_0=E_0/\omega^2$. The spatial orientation of the oscillations is specified by $\mathbf{e}_1$ and $\mathbf{e}_2$, unit vectors orthogonal to each other and to the propagation direction of the light, and $\delta=0$ corresponds to linear polarization and $\delta=\pm\pi/4$ to circular polarization. In a reference frame [Kramers-Henneberger (KH)] translated by $\alpha(t)$ with respect to the laboratory frame, the electrons no longer quiver, while, instead, the nucleus (considered infinitely heavier) quivers along the $\alpha(t)$ trajectory. In the KH frame, the Coulombic attraction between any electron and the nucleus takes the form $-Z/|\mathbf{r}_i+\alpha(t)|$, where Z is the nuclear charge.

The high-frequency Floquet theory (HFFT) pertains when the field frequency ω is high compared with the excitation energy of the atom in the field. Then, the electrons feel a time-averaged effective attractive potential, termed the "dressed potential," given by

$$V_0(\mathbf{r}_i, \alpha_0) = -\frac{Z}{2\pi}\int_0^{2\pi} \frac{d\Omega}{|\mathbf{r}_i + \alpha(\Omega/\omega)|}, \tag{2}$$

where $\Omega=\omega t$ and the average extends over one period of the laser field. The corresponding Schrodinger equation in the KH frame is

TABLE I. Parameters for the stability of atomic anions in superintense laser fields.

Quantity	D	Polarization[a]	H^-	H^{2-}	He^-	He^{2-}
α_0^{crit} (a.u.)	3	L	6	170	11	82
		C	6	250	4.3	51
	∞	L	3	181	3	59
		C	2.6	300	1.3	45
I^{crit} (10^{16} W/cm^2)	3	L	0.14	120	0.48	27
		C	0.29	501	0.15	21
	∞	L	0.036	130	0.06	14
		C	0.054	721	0.014	16
α_0^{max} (a.u.)	3	L	17	400	26	180
		C	16	600	14	140
	∞	L	10	500	12	160
		C	10	834	6	130
I^{max} (10^{16} W/cm^2)	3	L	1.2	640	2.7	130
		C	2.1	2900	1.6	160
	∞	L	0.4	1000	0.58	100
		C	0.8	5600	0.29	140
DE (eV)	3	L	1.1	0.026	1.2	0.12
		C	0.37	0.0073	1.1	0.078
	∞	L	1.2	0.019	1.4	0.14
		C	0.46	0.0052	1.1	0.066

[a]L and C denote linear and circular polarizations, respectively. Laser field intensity is related to photon frequency and quiver amplitude by $I=(1+\gamma^2)E_0^2/(2\mu_0 c_0)$, where γ is the polarization parameter, $\gamma=0$ for linear and $\gamma=1$ for circular. E_0; the intensity data given here pertain to $\omega=0.191$ a.u..

$$\sum_{i=1}^{N}\left[\frac{1}{2}p_i^2+V_0(\mathbf{r}_i,\alpha_0)+\sum_{j=1}^{i-1}\frac{1}{|\mathbf{r}_i-\mathbf{r}_j|}\right]\Phi=\epsilon(\alpha_0)\Phi. \tag{3}$$

Since the Hamiltonian is Hermitian, the energy eigenvalues, $\epsilon^{(N)}(\alpha_0)$ are real. The field parameters E_0 and ω appear only in the dressed potential and enter only via α_0, the quiver amplitude.

Of prime interest is the detachment energy required to remove one of the N electrons,

$$DE^{(N)}(\alpha_0)=\epsilon^{(N-1)}(\alpha_0)-\epsilon^{(N)}(\alpha_0). \tag{4}$$

As long as $DE>0$, the N-electron atom or ion remains stable with respect to the loss of an electron and thus supports at least one bound state. This stabilization requires $\alpha_0>\alpha_0^{crit}$, the critical quiver amplitude for which $DE=0$. At some higher value, denoted by α_0^{max}, DE reaches its maximum positive value, and as α_0 increases further DE eventually returns to zero. Table I reports our results for these and associated quantities, obtained from $D=3$ and large-D versions of HFFT applied to hydrogen or helium anions with $N=2,3,4$ in superintense high-frequency fields with linear or circular polarization.

III. EVALUATION FOR $D=3$

Our application of HFFT for $D=3$ employs well-known procedures.[11,16] For linear or circular polarizations, the dressed potential has an axis of cylindrical symmetry, taken as the z axis. For linear polarization, this axis is along the polarization direction; for circular polarization, it is along the propagation direction of the light. Thus, in the KH frame, for linear polarization the effective nuclear charge is spread along a segment between $\pm\alpha_0$ on the z axis, with most density near the end points. For circular polarization, the nuclear charge is uniformly distributed on a circle of radius α_0 in the xy plane with the center at $x=y=0$.

For linear polarization, it is convenient to use prolate spheroidal coordinates (ξ,η,ϕ) with foci located at $\pm\alpha_0$. The dressed potential $V_0(\mathbf{r}_i,\alpha_0)$ for each electron then takes the form

$$V_0(\mathbf{r}_i,\alpha_0)=-\frac{2Z}{\pi\alpha_0\sqrt{\xi_i^2-\eta_i^2}}K\left[\left(\frac{1-\eta_i^2}{\xi_i^2-\eta_i^2}\right)^{1/2}\right], \tag{5}$$

where $K(k)$ is the complete elliptic integral of the first kind. The wave functions and energy eigenvalues as functions of α_0 are obtained from Eq. (3) via standard self-consistent field methods. To evaluate the Hamiltonian matrix elements, we constructed one-electron orbitals using basis sets of 81 functions of the form

$$\Phi(\xi,\eta,\phi)_{p,q,m}=(\xi-1)^p\eta^q[(1-\eta^2)(\xi^2-1)]^{m/2}e^{-\gamma\xi}e^{im\phi}, \tag{6}$$

where p, q, and m are non-negative integers and γ is a variational parameter used to optimize the numerical results. As the starting approximation, the electrons ($N=2$, 3, or 4) were positioned at $z=\alpha_0$ and at equidistant points between; in the subsequent iterations, which converged rapidly to self-consistency, the overlap of the one-electron orbitals proved to be negligibly small. Accordingly, the Hartree-Fock exchange terms are likewise negligible, and since the Hamil-

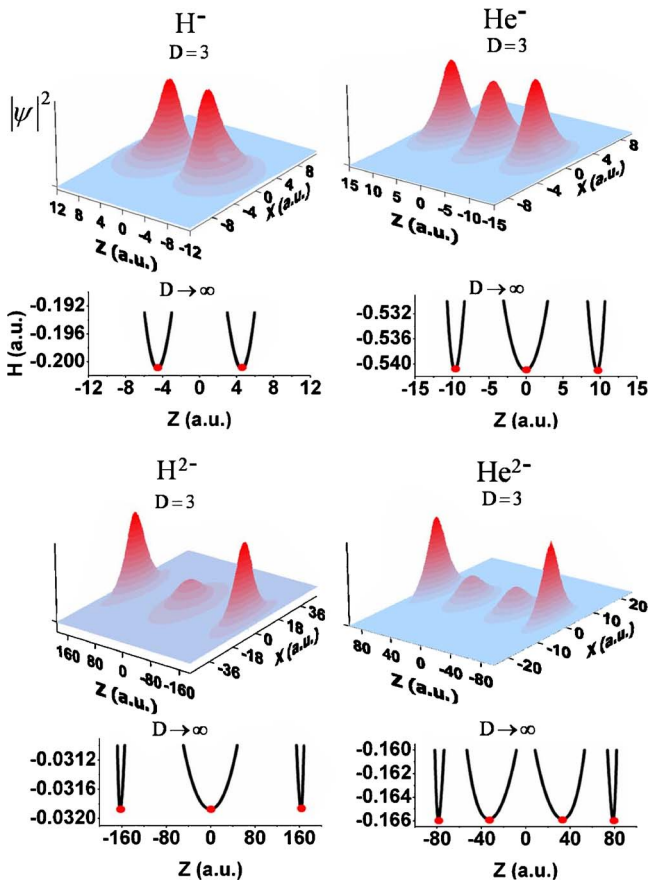

FIG. 1. (Color online) Electronic charge distributions for ground states of H^-, H^{2-}, He^-, and He^{2-} at critical values of the quiver amplitude, $\alpha_0^{\mathrm{crit}}=6$, 170, 11, and 82 a.u., respectively, for high-frequency superintense laser fields linearly polarized along the z axis. Upper panel shows probability densities obtained for $D=3$. Note that overlaps between lobes of $|\Psi|^2$ are negligibly small. The lower panel pertains to the large-D limit, showing cuts of the effective Hamiltonian of Eq. (10) along the z axis, evaluated for same values of the quiver amplitude. Dots at minima indicate the location of the electrons at the large-D limit.

tonian is independent of spin, the eigenvalues are degenerate with respect to spin.

Figure 1 displays the electronic charge distributions (upper panel) obtained for the ground states of H^-, H^{2-}, He^-, and He^{2-}, evaluated for critical values of α_0 just large enough to attain the onset of stabilization, where the detachment energy $DE^{(N)}(\alpha_0)$ of Eq. (4) becomes zero. The negligible overlap of the electron orbitals is evident, and when $\alpha_0 > \alpha_0^{\mathrm{crit}}$, the overlap decreases further. As shown in Fig. 2, the detachment energy then grows positive, thereby enabling the N-electron anion to support a bound state from which none of the electrons will autodetach.

For circular polarization, it is appropriate to use oblate spheroidal coordinates, and the dressed potential then has the form

$$V_0(\mathbf{r}_i,\alpha_0) = -\frac{2Z}{\pi\alpha_0(\xi_i+|\eta_i|)}K\left[\frac{2}{\xi_i+|\eta_i|}(\xi_i|\eta_i|)^{1/2}\right], \qquad (7)$$

where again $K(k)$ is the complete elliptic integral of the first kind. In contrast to the potential of Eq. (5), which is strongest near the line between $z=\alpha_0$, that of Eq. (7) is strongest in the vicinity of the circle $x^2+y^2=\alpha_0^2$. The basis sets employed in the self-consistent calculations have the form

$$\Psi_{p,q,m}(\xi,\eta,\varphi) = (\xi-1)^p\eta^q e^{-\gamma\xi}\begin{cases}\frac{1}{\sqrt{\pi}}\cos(m\varphi) & \text{if } m>0\\ \frac{1}{\sqrt{2\pi}} & \text{if } m=0\\ \frac{1}{\sqrt{\pi}}\sin(m\varphi) & \text{if } m<0,\end{cases} \qquad (8)$$

where the indices are related to familiar hydrogenic quantum

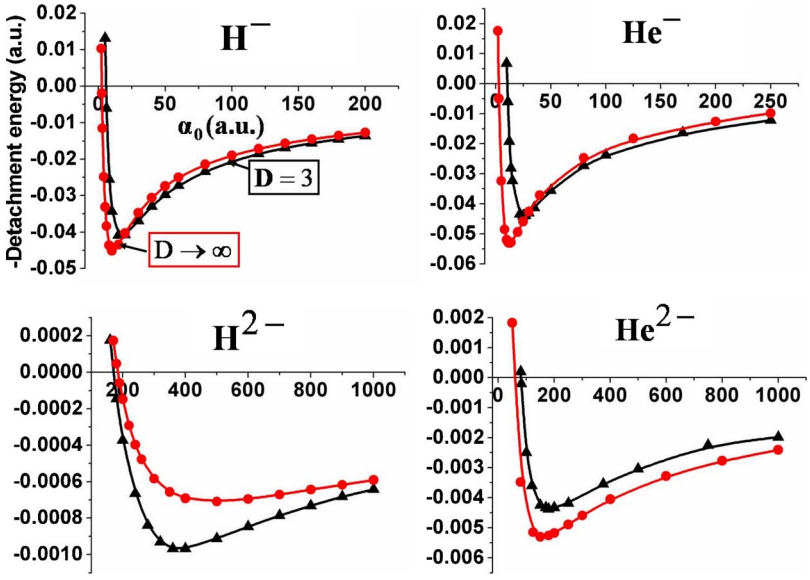

FIG. 2. (Color online) Negative of the detachment energy, $DE^{(N)}(\alpha_0)$, for the removal of an electron as a function of the quiver amplitude α_0 for the ground states of H^-, H^{2-}, He^-, and He^{2-} in the high-frequency limit of linearly polarized superintense laser fields. Results are shown for $D=3$ and the large-D limit. Table I lists quiver values, denoted as α_0^{crit} and α_0^{max}, that correspond to $DE^{(N)}=0$ and the maximum $DE^{(N)}$, respectively, together with corresponding laser intensities and the maximum detachment energies for both the $D=3$ and large-D limit.

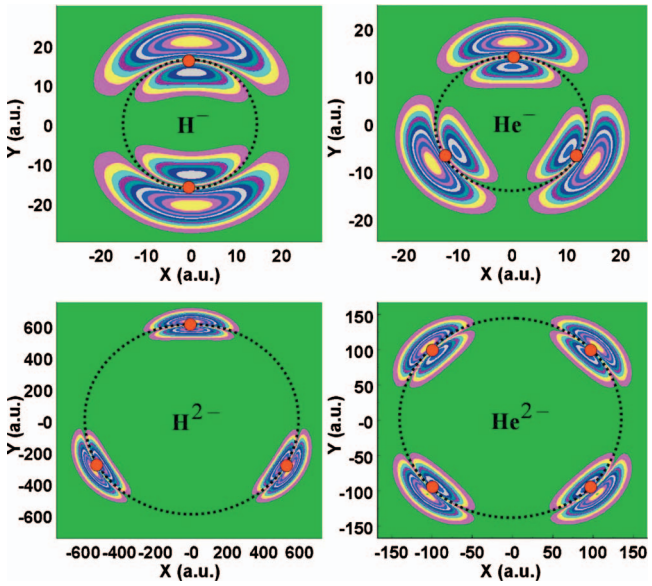

FIG. 3. (Color) Electronic charge distributions for ground states of H^-, H^{2-}, He^-, and He^{2-} in circularly polarized high-frequency superintense laser fields. Contours show probability densities for $D=3$; dots show positions of electrons for the large-D limit. Both contours and dots pertain to quiver amplitudes $\alpha_0^{max}=16$, 600, 14, and 140 a.u., respectively, corresponding to the maximum detachment energies for $D=3$.

numbers via $p=n-l-1$; $q=l-m$; and $m=-l,-l+1,\ldots,+l$. Again, γ is a variational parameter.

Figure 3 shows contour maps of the electronic charge distributions in the xy plane for ground states of the monoanions and dianions of hydrogen and helium. These pertain to values of α_0 that correspond to the maximum detachment energy. In each case, the distributions have an N-fold symmetry, with the electrons located in distinct lobes with peaks separated by $360/N$ deg. The lobes are all bimodal, comprised of a large component outside the circle of radius α_0 and a smaller companion inside the circle. This feature arises from the electron-electron repulsion term in Eq. (3), which pushes electrons as far apart as possible; the effect of that term is less pronounced for the dianions because for them α_0^{max} is much larger than for the monoanions. As seen in Fig. 4, the variation of detachment energies with α_0 for circular polarization is qualitatively similar to that in Fig. 2 for linear polarization. For a given magnitude of α_0^{max}, the corresponding detachment energy tends to be smaller for circular than for linear polarization.

IV. EVALUATION AT LARGE-*D* LIMIT

Dimensional scaling, as applied to electronic structure, involves generalizing the Schrodinger equation to D dimensions and introducing suitable D-scaled distance and energy units to remove the major, generic dimensional dependence.[14] Passing to the large-D limit then yields a pseudoclassical structure, in which the electrons are localized in the D-scaled space, at positions determined by the minimum of an effective Hamiltonian function. The latter contains no differential operators but comprises merely a centrifugal term, derived from the kinetic energy, in addition to the familiar Coulombic interactions of electrons and nuclei. As the scaling has removed most of the D dependence, the energy at the $D\rightarrow\infty$ limit, found simply as the minimum of the effective Hamiltonian, usually offers a good approximation to the $D=3$ energy.

This procedure provides a natural means to examine electron localization in a superintense laser field. In view of the axial symmetry that obtains for either linear or circular polarization, it is convenient to use D-dimensional cylindrical coordinates (akin to $x=\rho\cos\varphi$, $y=\rho\sin\varphi$ and z, in $D=3$); the Schrodinger equation in those coordinates is already available.[17] Because the essentially zero overlap among lobes of the electron distribution indicates that electron correlation can be neglected, we consider just the Hartree-Fock (HF) case.

For linear polarization, the large-D limit effective Hamiltonian corresponding to Eq. (3) then becomes

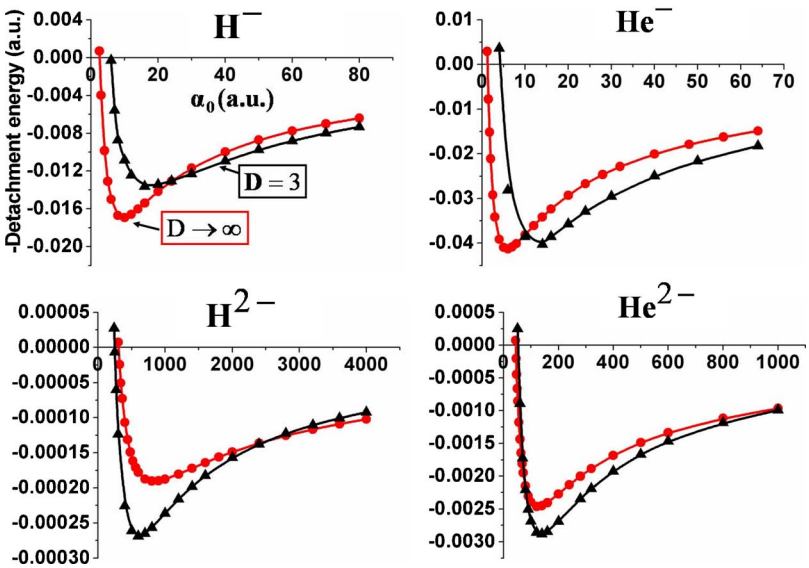

FIG. 4. (Color online) Negative of the detachment energy, $-DE^{(N)}(\alpha_0)$, for H^-, H^{2-}, He^-, and He^{2-}, as in Fig. 2, for the case of circularly polarized laser fields.

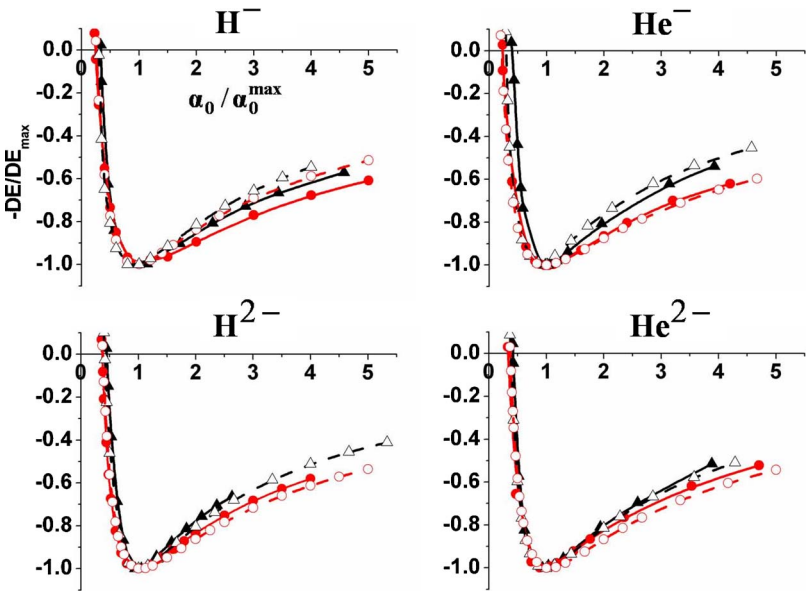

FIG. 5. (Color online) Scaled detachment energy functions, $-DE^{(N)}(\alpha_0)/DE^{(N)}(\alpha_0^{\max})$ plotted vs scaled quiver amplitudes, $\alpha_0/\alpha_0^{\max}$, for linearly (full symbols, full curves) and circularly (open symbols, dashed curves) polarized laser fields and for $D=3$ (triangles) and the large-D limit (circles). Table I lists the scaling parameters. Note the similarity in shapes of the curves for $D=3$ and the large-D limit, especially between the onset of stability (at α_0^{crit}) and the maximum of the detachment energy (at $\alpha_0^{\max}$).

$$\mathcal{H} = \frac{1}{2}\sum_{i=1}^{N}\frac{1}{\rho_i^2} + \sum_{i=1}^{N} V_0(\rho_i, z_i; \alpha_0) + \sum_{i=1}^{N}\sum_{j=i+1}^{N}\frac{1}{\sqrt{\rho_i^2+\rho_j^2+(z_i-z_j)^2}}, \tag{9}$$

where for the ith electron, ρ_i measures the distance from the polarization axis, z_i is the distance along that axis, and the dressed electron-nucleus interaction is given by

$$V_0(\rho_i, z_i; \alpha_0) = \frac{-Z}{2\pi}\int_0^{2\pi}\frac{d\Omega}{\sqrt{\rho_i^2+(z_i+\alpha_0\sin\Omega)^2}}. \tag{10}$$

All distance coordinates, including α_0, are scaled by κ^2 and energies by $1/\kappa^2$, with $\kappa=(D-1)/2$; thus, $\kappa=1$ at $D=3$. In Eq. (9), the first term is the centrifugal contribution. The third term is the $1/r_{ij}$ electron-electron repulsion; in the HF case, its form is simplified because the dihedral angle between any pair of electrons $\varphi_i-\varphi_j=90°$ in the large-D limit.[18] By minimizing Eq. (9) we obtain the energy $\epsilon_\infty^{(N)}$ as well as the positions of the localized electrons as functions of α_0. The calculations required are thus far easier to perform than for $D=3$. As seen in Figs. 1 and 2 and Table I, the results we find for $D\to\infty$ compare fairly well with those for $D=3$. Particularly for the quantity of chief experimental interest, the variation of detachment energy with α_0, the large-D limit appears to offer adequate estimates.

For circular polarization, we used the same procedure except for reorienting the quiver amplitude. The effective HF Hamiltonian for the large-D limit then takes the same form as Eq. (9) except that the dressed potential is replaced by

$$V_0(x_i, y_i, z_i; \alpha_0) = \frac{-Z}{2\pi}\int_0^{2\pi}\frac{d\Omega}{\sqrt{z_i^2+(x_i+\alpha_0\cos\Omega)^2+(y_i+\alpha_0\sin\Omega)^2}}. \tag{11}$$

Again, as seen in Figs. 3 and 4 and Table I, the large-D results compare well with those obtained for $D=3$; the electrons localize at angular intervals of $2\pi/N$, at the corners of an N-sided polygon inscribed in the circle of polarization.

V. DISCUSSION

In the HFFT domain, both the blossoming of the electron distribution into distinct lobes, seen in Figs. 1 and 3, and the variation of the detachment energy with quiver amplitude, seen in Figs. 2 and 4, exhibit a qualitative resemblance to a molecular structure. Figure 5 displays a further aspect. There, the $DE(\alpha_0)$ curves are normalized by scaling both DE and α_0 to their values at the maximum detachment energy. These scaled curves become quite similar for the four anions considered and for linear and circular polarizations, especially in the region between the onset of stability and the maximum detachment energy.

Thus, $DE(\alpha_0)$ emulates a potential energy curve for the stretching of a chemical bond, although $DE^{\max}$ is much

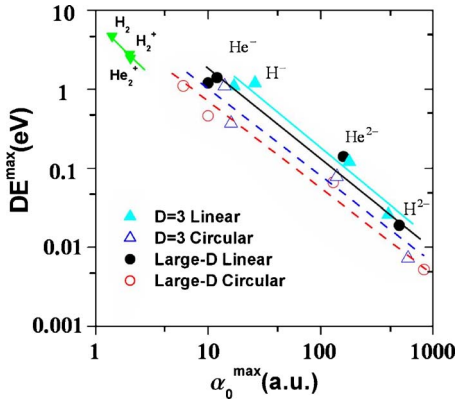

FIG. 6. (Color online) Log-log plot of maximum detachment energy, $DE^{\max}$ (eV), as a function of corresponding quiver amplitude, $\alpha_0^{\max}$ (a.u.), for the four atomic anions of Fig. 4, using again full symbols and full lines for linearly polarized and open symbols and dashed lines for circularly polarized laser fields, triangles for $D=3$, and circles for the large-D limit. For comparison, the upper left-hand corner includes the plot of bond dissociation energies vs bond lengths for the molecules H_2, H_2^+, and He_2^+ in field-free, $D=3$ space.

smaller than typical bond dissociation energies and $\alpha_0^{\max}$ is much larger than equilibrium bond lengths. Figure 6 shows that, on a log-log plot, the correlation between $DE^{\max}$ and $\alpha_0^{\max}$ is actually similar to, but not as steep, as that between the bond dissociation energies and bond lengths for H_2, H_2^+, and He_2^+ molecules. The correlation for $DE^{\max}$ extends over three orders of magnitude and is much the same for linear and circular polarizations and whether for $D=3$ or the large-D limit. We find also that HFFT results[11] obtained at $D=3$ for Li^- and Li^{2-} likewise conform to this plot.

The use of the HFFT is subject to three validity criteria.[15] (1) The dipole approximation requires the wavelength of the field to be large compared to $2\alpha_0$, for either linear or circular polarization. For the frequency, this specifies $\omega \ll 137\pi/\alpha_0$. (2) Further, the maximum quiver speed of the electrons must be much smaller than the speed of light. That requires $\alpha_0\omega \ll 137$; so, whenever this nonrelativistic constraint holds, so does the dipole approximation. (3) To attain the high-frequency regime, the field must oscillate much faster than electron motion within the atom. This requires that $|\epsilon^{(N)}(\alpha_0)| \ll \omega$. For instance, the ultrahigh power KrF laser provides photons with $\omega=0.19$ a.u. (5 eV). For the four anions of Table I, this ω would satisfy the lower bound (3) but the upper bound (2) would in the H^{2-} case not be sustained because α_0^{crit} is too large.

We obtained from the large-D limit version of HFFT a modest accuracy with far simpler computations than conventional $D=3$ methods. D-scaling treatments should prove useful for exploratory studies of other superintense laser processes, particularly involving electron localization. Inviting opportunities akin to our present study include examining the shapes of electron distributions induced by further varieties of laser polarization (e.g., elliptical, tetrahedral) or by multichromatic[10] rather than monochromatic radiation. The large-D limit will also facilitate the evaluation of HFFT for molecules and the incorporation of time dependence. When necessary, results can be systematically improved by the use of a $1/D$ perturbation expansion.[19]

The almost total lack of experimental evidence for the inhibition of ionization in a high-frequency superintense laser field looms in marked contrast with the abundance of theoretical work affirming and elucidating stabilization. Many discussions emphasize, among other experimental challenges, a daunting aspect.[12] In order to attain the requisite intensity, a pulsed laser must be used. During the rising edge of the pulse, the target atoms or anions will be ionized. Few if any may survive intact when the pulse intensity has reached the stabilization regime. This is termed the "death valley" problem. It is generally regarded as the key reason that stabilization has remained experimentally so elusive. The only exception, as yet, involved a Rydberg atomic state, enable to survive death valley because the minimum lifetime for ionization exceeded the pulse rise time.[12] We expect that the use of the large-D limit will aid a search, guided by theory, to identify similar cases amenable to an experimental observation of stabilization.

ACKNOWLEDGMENTS

We are grateful for support of this work by the Army Research Office and by a Department of Energy BES grant (DE-FG2-01ER15197). We also thank Marlan Scully for the opportunity to attend his Casper workshop, supported by the Institute for Quantum Studies at Texas A&M, where we recognized the virtues of treating the HFFT in the large-D limit.

[1] H. S. Massey, *Negative Ions*, 3rd ed. (Cambridge University Press, London, 1976).
[2] M. K. Scheller, R. N. Compton, and L. S. Cederbaum, Science **270**, 1160 (1995).
[3] S. Kais and P. Serra, Adv. Chem. Phys. **125**, 1 (2003).
[4] A. Dreuw and L. S. Cederbaum, Chem. Rev. (Washington, D.C.) **102**, 181 (2002).
[5] S. N. Schauer, P. Williams, and R. N. Compton, Phys. Rev. Lett. **65**, 625 (1990).
[6] X. B. Wang and L. S. Wang, Phys. Rev. Lett. **83**, 3402 (1999).
[7] Q. She and S. Kais, J. Am. Chem. Soc. **124**, 11723 (2002).
[8] For an overview of superintense high-frequency phenomena, treated with the high-frequency Floquet theory, see M. Gavrila, in *Atoms in Super Intense Laser Fields*, edited by M. Gavrilla (Academic, New York, 1992), p. 435.
[9] J. H. Eberly and K. C. Kulander, Science **262**, 1229 (1993).
[10] E. van Duijn, M. Gavrila, and H. G. Muller, Phys. Rev. Lett. **77**, 3759 (1996).
[11] Q. Wei, S. Kais, and N. Moiseyev, J. Chem. Phys. **124**, 201108 (2006).
[12] N. J. van Druten, R. C. Constantinescu, J. M. Schins, H. Nieuwenhuize, and H. G. Muller, Phys. Rev. A **55**, 622 (1997); M. P. de Boer, J. H. Hoogenraad, R. B. Vrijen, R. C. Constantinescu, L. D. Noordam, and H. G. Muller, *ibid.* **50**, 4085 (1994).
[13] N. Moiseyev and L. S. Cederbaum, J. Phys. B **32**, L279 (1999).
[14] D. R. Herschbach, J. Avery, and O. Goscinski, *Dimensional Scaling in Chemical Physics* (Kluwer, Dordercht, 1993).
[15] E. van Duijn and H. G. Muller, Phys. Rev. A **56**, 2182 (1997).
[16] M. Pont, N. R. Walet, M. Gavrila, and C. W. McCurdy, Phys. Rev. Lett. **61**, 939 (1988).
[17] D. D. Frantz and D. R. Herschbach, Chem. Phys. **126**, 59 (1988).
[18] D. Z. Goodson and D. R. Herschbach, J. Chem. Phys. **86**, 4997 (1987).
[19] B. A. McKinney, M. Dunn, D. K. Watson, and J. G. Loeser, Ann. Phys. **310**, 56 (2004).